A Simple Algorithm for Defect Detection From a Few Radiographies

Lionel Fillatre, Igor Nikiforov and Florent Retraint

Institut Charles Delaunay (ICD - FRE CNRS 2848)
Université de Technologie de Troyes
Troyes, France
Email: {lionel.fillatre, igor.nikiforov, florent.retraint}@utt.fr

***Abstract*— The paper concerns the radiographic non-destructive testing of well-manufactured objects. The detection of anomalies is addressed from the statistical point of view as a binary hypothesis testing problem with non-linear nuisance parameters. A new simple and numerically stable detection scheme is proposed as an alternative to the conventional generalized likelihood ratio test which becomes untractable in the non-linear case. This original decision rule detects the anomalies with a loss of a negligible part of optimality with respect to an optimal test designed for the "closest" hypothesis testing problem with linear nuisance parameters. The inspection of nuclear fuel rods is discussed to illustrate the relevance of the proposed theoretical solution.**

***Index Terms*— Anomaly detection, Parametric tomography, Statistical hypotheses testing, Nuisance parameter, Non-destructive testing.**

I. Introduction

The Quantitative Non-Destructive Testing (QNDT) of industrial equipment components is a crucial issue to warrant the quality of manufacturing objects. Particularly, in the nuclear fuel rod inspection, it is desirable to detect defects, inclusions or any unexpected cavities to assure the safety and reliability of installations. X-ray examination is a commonly used method for detecting internal welding flaws. It is based on the ability of X-rays to pass through metals and other materials opaque to ordinary light, and to produce photographic records by the transmitted radiant energy.

In many industrial applications, conventional computed tomographic techniques are intractable or expensive owing to constraints of time, dimensions and the type of material to be inspected. A solution based on the use of an X-ray radiographic chain providing a small number of radiographs offers more flexibility. Unfortunately, since the number of projections and/or view angles available for inspection is very limited, the full pixel-by-pixel reconstruction of the inspected object becomes impossible and the detection of defects is very difficult.

The proposed solution of the defect detection problem is based on the assumption that the imaged medium is composed of an (partially) unknown non-anomalous background, which is considered as a non-random nuisance parameter, with a possibly hidden anomaly (informative parameter). The non-anomalous background is considered as a nuisance parameter because the QNDT inspectors are essentially interested in detecting defects but the negative impact of the non-anomalous background on the decision making process is not negligible.

To counterbalance the lack of observations in the case of a few projections it is proposed to use a non-linear parametric parsimonious model of the non-anomalous background. The defect detection is considered as a parametric hypotheses testing problem between two composite alternatives with non-linear nuisance parameters. The Generalized Likelihood Ratio (GLR) test [1], [2], which is usually used to solve this kind of problem, has three major drawbacks : 1) the optimality of the GLR is established only asymptotically, i.e. when the number of observations is very large, but it is often suboptimal for a limited number of observations ; 2) the GLR test requires the estimation of unknown parameters before taking a decision, which becomes untractable in the non-linear case and 3) the GLR scheme makes no distinction between non-linear and linear parts of parametric model. In the above mentioned radiographic inspection problem, the imperfections of X-ray attenuation properties of the non-anomalous background define a linear part of the model and the geometrical imperfections define a non-linear one. Splitting the geometric and physical factors permits the model to be simplified. Hence, instead of untractable solution based on the GLR test, suffering from serious numerical problems (poor and unstable convergence of the minimization process and a high sensitivity of the solution to initial conditions), another more tractable solution is proposed in the paper. This simple and numerically stable detection scheme detects anomalies with a loss of a negligible part of optimality with respect to an optimal test designed for a reference model of non-anomalous background with perfectly known geometrical factors.

The paper is organized as follows. Section II is devoted to the statement of practical problem : the nuclear fuel rod inspection. A brief overview of the inspection procedure main steps is described. Next, the conventional methods of radiographic inspection and the main contribution of the paper are discussed in section III. The parsimonious parametric model of the inspected object and radiographic process is presented in section IV. Unfortunately, the ob-

tained measurement model is non-linear. The basic principle of statistical detection is presented and the limits of the non-linear GLR test are discussed in section V. Instead of untractable solution based on the non-linear GLR test, another more tractable solution is proposed in section VI. A special attention is paid to the numerical aspects of the problem and a detailed flowchart of detection algorithms is also described here. Some experimental results with real radiographies illustrating the relevance of the proposed theoretical solution are shown in section VII. Finally, some concluding remarks are drawn in section VIII.

II. Defect detection overview

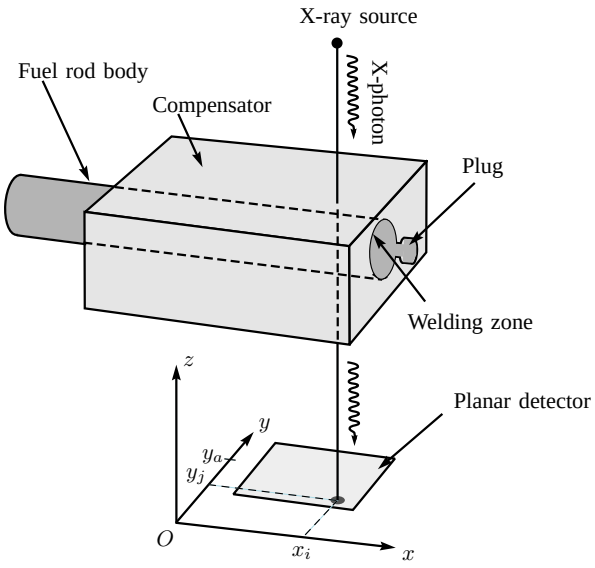

Fig. 1. Geometry of the nuclear fuel rod inspection system.

A nuclear fuel rod is composed of a body and a plug as shown in Figure 1 [3]. The body is manufactured separately from the plug and, before its use, the plug is welded with the body. The goal of the nuclear fuel rod inspection is to detect defects (anomalies) in the welding zone which corresponds to a tangential part of the fuel rod (see Figure 1). Through the inspection procedure, the nuclear fuel rod is imaged with a tomographic system composed of an X-ray source and a planar detector. The fuel rod is put into a compensator which is made of the same material to avoid the high contrast of radiography near the edges of the fuel rod. The goal is to decide between the two possible situations : $\mathcal{H}_0 = \{$there is no anomaly in the welding zone$\}$ and $\mathcal{H}_1 = \{$there is an anomaly in the welding zone$\}$.

Figure 2 shows the major steps of the proposed welding defect detection procedure. The first step consists in acquiring the radiography of the inspected object. The second step is devoted to the automatic selection of the region of interest corresponding to the welding zone. It is possible since the inspected object is well positioned in the radiographic system support. The third

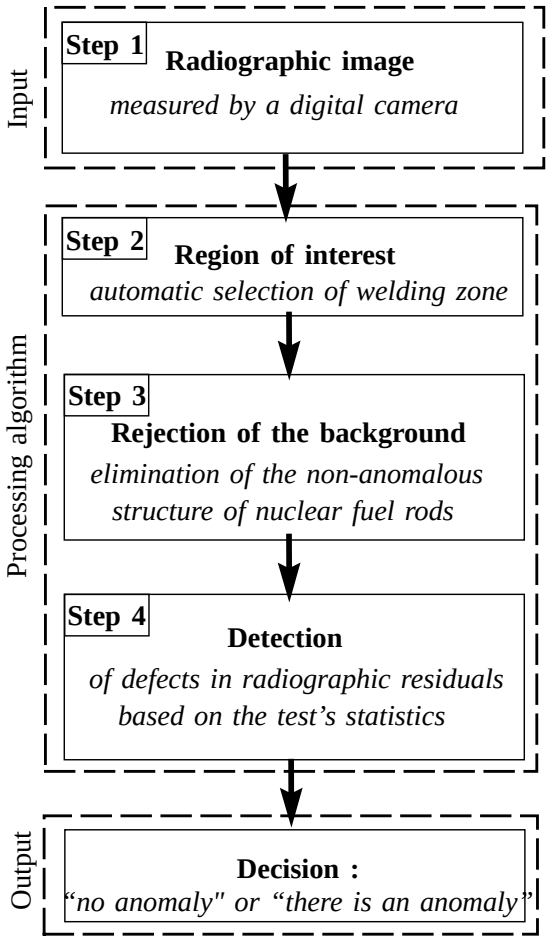

Fig. 2. Procedure for the detection of defects.

step corresponds to the rejection of nuisance parameters, i.e. the rejection of the non-anomalous background of the fuel rod from the radiography to compute the residuals. Theoretically, the residuals are completely free from the non-anomalous nuclear fuel rod structures and they can be potentially corrupted only by a random measurement noise and by defects. The fourth step is devoted to the computation of the test's statistics and to the comparison of this statistics with a given threshold. If the computed value of statistics exceeds the threshold, an anomaly is declared.

III. Related works and contribution of the paper

First, the state of the art is presented. Next, the advantages and disadvantages of Bayesian and non-Bayesian approaches are discussed. Finally, the motivation and the contribution of the paper are described.

A. The state of the art

Existing methods for detecting internal defects in radiographies [4] fall into three groups : 1) methods without

a priori knowledge, 2) reference methods and 3) Computerized Tomography (CT) methods. The actual paper belongs to this last group.

The first group includes the methods of defect detection without prior knowledge of the imaged media structures, i.e. the methods without (statistical) model. Such approaches typically use the image processing tools (for example, field flattening to enhance the contrast) [5], pattern recognition [6], expert systems [7] and artificial neural networks [8], [9]. The prerequisite for these methods is the existence of common properties which consistently define all kinds of anomalies and distinguish them from the character features of the non-anomalous imaged media [4], [10], [11]. Often, these methods are noise-sensitive since they do not include explicitly a random noise in the measurement model.

In the second group, it is assumed that a reference radiography (model) [4] is available. If a significant difference is identified by comparing the tested image with a reference one [12], then the inspected piece is classified as defective. This approach is efficient to deal with a well-known inspected piece but it is heavily based on a reference model, which is not always possible in practice.

The third group (CT methods) consists in detecting defects from radiographies by reconstructing the imaged media, which are composed of an (partially) unknown non-anomalous background with possibly hidden defects. Since the number of projections and/or angles of view available for inspection is very limited and the pixel-by-pixel reconstruction is impossible [13], the introduction of prior information on the unknown background is inevitable to fill up the gap in the missing data.

Two methods of prior information introduction are available in the literature according to their nature : deterministic and statistical. A purely deterministic regularization [14] of this ill-posed problem [15] has some drawbacks including artifacts in the resulting image and noise sensitivity among others. The statistical CT approaches to anomaly detection can be divided into two groups : Bayesian and non-Bayesian. The dominant trend in the literature is the Bayesian statistical approach [14], [16]–[19]. In the case of anomaly detection problem, it is assumed that : i) the considered hypotheses, $\mathcal{H}_0 =$ {the inspected object is defect-free} and $\mathcal{H}_1 =$ {the inspected object contains defects}, are random events with known prior probabilities ; ii) the non-anomalous background (or its structure) and the anomalies are random and the parameters of their (usually Gaussian) *a priori* distribution are known. In this paper, which continues our previous publication [20], [21], another, non-Bayesian, statistical philosophy is adopted : it is assumed that the non-anomalous background is a non-random nuisance parameter. If the geometrical and/or physical properties of the inspected objects cannot be described by an *a priori* known probabilistic model then a more convenient working hypothesis about the non-anomalous object is the assumption that its geometrical and/or physical properties are non-random unknown nuisance parameter. Often, this is the case in the QNDT of industrial equipment components, in welding defects detection for instance.

B. Motivation and contribution of this paper

The main objective of the paper is to solve the anomaly detection problem by using a simple and numerically stable detection algorithm with reliable statistical performances. A key assumption is the existence of a parametric model of the non-anomalous background (physical/geometrical properties of the nuclear fuel rods). The non-destructive inspection problem is formalized as a binary statistical decision with unknown nuisance parameters. The main issue of such a decision problem is its ability to detect an anomaly while being insensitive to the nuisance parameters. Such a parametric model makes possible, by using a nuisance rejection technique, to find a subspace of the observation space, where the impact of the non-anomalous background is absent or negligible. Because the physical/geometrical properties of the inspected manufactured objets are usually standardized and, hence, a relatively simple parametric model can be developed, the approach proposed in this paper seems to be particularly promising in QNDT. Some examples of such a background defined by deterministic functions have been previously discussed in [9], [22]. Also a rudimentary version of the background rejection technique, i.e. the field-flattening operation [5], whose goal is to enhance the anomaly contrast in radiographies by eliminating the variations of contrast provoked by the background is widely used in QNDT. Unfortunately, the obtained parametric model is non-linear which seriously compromise the numerical stability of the GLR test. Finally, to overcome the numerical problems and to design a stable and numerically efficient detection algorithm the geometric and physical factors have been separated to simplify the parametric model of non-anomalous background. This numerically stable algorithm detects anomalies with a loss of a negligible part of optimality with respect to an optimal test designed for a reference model of non-anomalous background with perfectly known geometrical factors.

IV. Measurement model

This section briefly describes a parsimonious parametric model of the nuclear fuel rods inspection procedure. Both, the model of non-anomalous welding zone, $\mathcal{H}_0$, and the model of anomalous welding zone $\mathcal{H}_1$ are described here.

A. Scalar measurement model

To simplify the problem, the parallel-beam geometry is used in the paper and the X-rays are all oriented along the z-axis (see Figure 1). The planar detector coincides with the xOy-plane. The measurements $\zeta(x, y)$ at different

points (x, y) of the detector are modeled as independently distributed random variables [23] such that :

$$\zeta(x,y) \sim \begin{cases} \Pi(m(x,y)) & \text{under} \quad \mathcal{H}_0 \\ \Pi(\theta(x,y)+m(x,y)) & \text{under} \quad \mathcal{H}_1 \end{cases} \quad (1)$$

where $\Pi(m)$ denotes the Poisson law with parameter $m > 0$. The *unknown* quantity $m(x, y)$ represents the mean number of photons passing through a defect-free media at the position (x, y) and $\theta(x, y)$ represents the local variation of the mean number of X-photons arrived on the planar detector due to a defect at the position (x, y). It is assumed that

$$m(x,y) = \mu(x,y) + \omega(x,y) \quad (2)$$

where the *unknown* quantity $\mu(x, y)$ (resp. $\omega(x, y)$) represents the mean number of photons passing through the media (resp. the mean number of extra photons, caused primarily by scattered radiations) at the position (x, y).

Let r be the radius of the fuel rod and $l(x, y; r)$ be the material (the fuel rod together with the compensator) thickness corresponding to the location (x, y) on the detector (see Figure 1). It is assumed that an unknown value of r belongs to the interval $I = [r_0 - \varrho; r_0 + \varrho]$, where ϱ is a small positive constant and r_0 is exactly known. The region of interest $\mathcal{R}$ is defined by the couples $(x, y) \in \mathbb{R}^2$ such as

$$\mathcal{R} = \{(x,y) \mid x_{\min} \le x \le x_{\max}\,, y_{\min} \le y \le y_{\max}\} \quad (3)$$

where the bounds $x_{\min}$, $x_{\max}$, $y_{\min}$ and $y_{\max}$ are precisely known. Let y_a be the y-coordinate of the fuel rod revolution axis on the xOy-plane (see Figure 1). A short calculus shows that the material thickness $l(x, y; r)$ crossed by the X-ray beam arriving at the location (x, y) on the detector belonging to the region of interest, i.e. $y_a - y < r_0 - \varrho$ (see Figure 1), is a sum of two terms : $l(x, y; r) = l_r(x, y; r) + l_c(x, y)$, where

$$l_r(x,y;r) = \sqrt{r^2 - (y_a - y)^2} \quad (4)$$

is the rod material thickness corresponding to the location (x, y) on the detector and $l_c(x, y)$ is the exactly known compensator thickness.

It is assumed that the quantity $\mu(x, y)$ can be well approximated [24] by the polynomial function :

$$\mu(x,y) \approx \widehat{\mu}(x,y;r,a_0,\mathbf{a}) = a_0 + \sum_{k=1}^{n_{\mathbf{a}}} a_k\, l^k(x,y;r), \quad (5)$$

where $\mathbf{a} = (a_1\ a_2\ \ldots\ a_{n_{\mathbf{a}}})^T$ is the vector of coefficients, and the impact of scattered radiations can be approximated by a bivariate polynomial function :

$$\omega(x,y) \approx \widehat{\omega}(x,y;\mathbf{b}) = \sum_{u=0}^{n_u}\sum_{v=0}^{n_v} b_{u,v} x^u y^u, \quad (6)$$

where $\mathbf{b} = (b_{0,0}\, b_{1,0}\ \ldots\ b_{n_u,n_v})^T$. To avoid the redundancy with the term $b_{0,0}$ in (6), the term a_0 from (5) is omitted in the rest of the paper. It is assumed that the vector $\mathbf{a}$ belongs to a compact set $K_{\mathbf{a}} \subset \mathbb{R}^{n_{\mathbf{a}}}$ and the vector $\mathbf{b}$ belongs to a compact set $K_{\mathbf{b}} \subset \mathbb{R}^{n_{\mathbf{b}}}$ with $n_{\mathbf{b}} = (n_u + 1)(n_v + 1)$ to warrant the validity of the approximation given by (5) and (6).

Moreover, for the considered problem, the exposure time and the X-flux intensity are high enough to warrant a good signal-to-noise ratio. Consequently, the Gaussian approximation of the Poisson distribution is relevant, which leads to a more tractable detection problem when anomalies are unspecified. Hence, by considering (5) and (6), the measurement model (1) is approximated by the following one :

$$\zeta(x,y) = \begin{cases} \widehat{m}(x,y;\mathbf{c}) + \xi(x,y) \text{ under } \mathcal{H}_0 \\ \theta(x,y) + \widehat{m}(x,y;\mathbf{c}) + \xi(x,y) \text{ under } \mathcal{H}_1 \end{cases} \quad (7)$$

with $\widehat{m}(x,y;\mathbf{c}) = \widehat{\mu}(x,y;r,\mathbf{a}) + \widehat{\omega}(x,y;\mathbf{b})$, $\mathbf{c} = (r, \mathbf{a}, \mathbf{b}) \in K$, $K = I \times K_{\mathbf{a}} \times K_{\mathbf{b}} \subset \mathbb{R}^{n_{\mathbf{c}}+1}$, $n_{\mathbf{c}} = n_{\mathbf{a}} + n_{\mathbf{b}}$ and $\xi(x, y) \sim \mathcal{N}(0, \sigma^2(x, y))$. The standard deviation $\sigma(x, y)$ is defined by (see [25, p. 285-288]) :

$$\sigma(x,y) = \eta(\bar{m}(x,y))^{\frac{1}{2}}, \quad (8)$$

where $0 \le \eta \le 1$ is a known experimental coefficient independent of (x, y) and $\bar{m}(x, y)$ is an experimental mean value for $m(x, y)$. Since defects essentially change the mean of the measurements, the quality of the estimate $\sigma(x, y)$ is not crucially important for the detection.

B. Vector measurement model

The planar detector, which is composed of $n = n_x\, n_y$ discrete sensors, can be viewed as a $n_x \times n_y$ matrix. Let $\zeta_{i,j}$ (resp. $\theta_{i,j}$ and $\xi_{i,j}$) denotes the quantity $\zeta(x_i, y_j)$ (resp. $\theta(x_i, y_j)$ and $\xi(x_i, y_j)$) defined for the i, j-th node of this "discrete" planar detector (see Figure 1). Let $\Xi = \mathrm{vec}(\{\zeta_{i,j}\})$ be the lexicographical ordering of measurements $\zeta_{i,j}$. A bit of algebra shows that :

$$M(\mathbf{c}) = \mathrm{vec}(\{\widehat{m}(x_i,y_j;\mathbf{c})\}) = F(r)\mathbf{a} + G\mathbf{b}, \quad (9)$$

where

$$F(r) = (F_1(r)\ \ldots\ F_{n_{\mathbf{a}}}(r)) \quad (10)$$

is an $n \times n_{\mathbf{a}}$ matrix,

$$G = (G_1\ \ldots\ G_{n_{\mathbf{b}}}) \quad (11)$$

is an $n \times n_{\mathbf{b}}$ matrix, $F_s(r) = \mathrm{vec}(\{l^s(x_i, y_j; r))\})$ for $1 \le s \le n_{\mathbf{a}}$, $G_k = \mathrm{vec}\big(\{x_i^u y_j^v\}\big)$ such as $k = u\,(n_v + 1) + v + 1$. Hence, the above approximated measurement model (7) can be rewritten :

$$\mathbf{y} = \Sigma^{-\frac{1}{2}}\,\Xi = \begin{cases} H(\mathbf{c}) + \boldsymbol{\xi} & \text{under} \quad \mathcal{H}_0 \\ \boldsymbol{\theta} + H(\mathbf{c}) + \boldsymbol{\xi} & \text{under} \quad \mathcal{H}_1 \end{cases}, \quad (12)$$

where $\boldsymbol{\theta} = \Sigma^{-\frac{1}{2}}\mathrm{vec}(\{\theta_{i,j}\})$, $H(\mathbf{c}) = \Sigma^{-\frac{1}{2}}\,M(\mathbf{c})$, $\boldsymbol{\xi} = \Sigma^{-\frac{1}{2}}\mathrm{vec}(\{\xi_{i,j}\})$ and $\Sigma^{-\frac{1}{2}}$ is a diagonal $n \times n$ matrix. The lexicographically ordered diagonal elements

$$\Sigma^{-\frac{1}{2}} = \mathrm{diag}\left\{\mathrm{vec}\big(\{\sigma^{-1}(x_i,y_j)\}\big)\right\} \quad (13)$$

are computed by using (8) for (x_i, y_j) taking in the lexicographical order. The random vector $\boldsymbol{\xi} \sim \mathcal{N}(0, I_n)$ follows the n-dimensional Gaussian law with a zero mean and the identity covariance matrix I_n.

V. Principle of statistical detection

This section is devoted to the anomaly detection considered as a statistical hypotheses testing with nuisance parameters. First, the non-linear model of nuisance parameters is examined. It is shown that the application of the non-linear GLR test meets serious obstacles.

A. Statistical hypotheses testing

The hypotheses testing problem consists in deciding between the two following hypotheses

$$\mathcal{H}_0 = \{\mathbf{y} \sim \mathcal{N}(\boldsymbol{\theta} + H(\mathbf{c}), I_n);\ \boldsymbol{\theta} = 0,\ \mathbf{c} \in K\} \quad (14)$$

and

$$\mathcal{H}_1 = \{\mathbf{y} \sim \mathcal{N}(\boldsymbol{\theta} + H(\mathbf{c}), I_n);\ \boldsymbol{\theta} \neq 0,\ \mathbf{c} \in K\}. \quad (15)$$

The quality of a statistical test is defined with a set of error probabilities, namely : "false alarm" and "non detection" [26], [27]. The false alarm means that a non-anomalous welding zone has been declared by the inspection procedure as a zone with defects. Let α be the probability of this event. The non detection occurs when a defective welding zone is declared as a non-anomalous one. Let $1-\beta$ be the probability of non detection. The probability β is called the power of the test. It corresponds to the probability to declare an alarm when the inspected zone contains defects.

The subtlety of the above mentioned hypotheses testing problem consists in the existence of the unknown non-linear nuisance parameter $\mathbf{c}$. As it has been mentioned before, distinguishing two subsets of parameters, the parameters of interest (anomaly) $\boldsymbol{\theta}$ and the nuisance parameter (non anomalous media) $\mathbf{c}$, is necessary because the nuisances parameters are of no interest for inspection. The performance indexes (α, β) of statistical tests are functions of both the parameter of interest $\boldsymbol{\theta}$ and the nuisance parameters $\mathbf{c}$. The desirable relation between the performance indexes (α, β) of a test and the parameter of interest $\boldsymbol{\theta}$ usually results from the application and the statistical nature of the problem, in order to achieve optimal properties of the test. But there is no desirable relation between (α, β) and the nuisance parameter $\mathbf{c}$, the goal is to achieve the performance indexes independent of the actual value of $\mathbf{c}$.

To summarize the decision problem statement, the power function $\beta(\delta; \boldsymbol{\theta}, \mathbf{c}) = \Pr_{\boldsymbol{\theta}\neq 0, \mathbf{c}}(\delta(\mathbf{y}) = \mathcal{H}_1)$ is defined, where the probability $\Pr_{\boldsymbol{\theta},\mathbf{c}}$ stands for the vector of observations $\mathbf{y}$ being generated by the distribution $\mathcal{N}(\boldsymbol{\theta} + H(\mathbf{c}), I_n)$. With these notations, the quantity $\alpha(\delta) = \sup_{\mathbf{c}} \Pr_{\boldsymbol{\theta}=0,\mathbf{c}}(\delta(\mathbf{y}) = \mathcal{H}_1)$ corresponds to the worst probability of false alarm, while considering $\mathbf{c}$ as an unknown vector. Roughly speaking, the power function $\beta(\delta; \boldsymbol{\theta}, \mathbf{c})$ should be as large as possible for every $\boldsymbol{\theta} \neq 0$ and $\mathbf{c}$, for a prescribed probability of false alarm $\alpha(\delta) = \alpha$. Interested reader can found a detailed discussion of statistical issues in relation with the anomaly detection procedure in [20], [21], [28], [29].

B. Limits of the non-linear GLR test

Because a non-linear character of the function $\mathbf{c} \mapsto H(\mathbf{c})$, an immediate application of invariant tests [21] is compromised. At first glance, the only solution to overcome the above-mentioned difficulty is to utilize the GLR test, which is applicable without any prerequisites :

$$\widehat{\delta}(\mathbf{y}) = \begin{cases} \mathcal{H}_0 \text{ if } \widehat{\Lambda}(\mathbf{y}) = \dfrac{\sup_{\boldsymbol{\theta}\neq 0, \mathbf{c}\in K} f_{\boldsymbol{\theta}+H(\mathbf{c})}(\mathbf{y})}{\sup_{\mathbf{c}\in K} f_{H(\mathbf{c})}(\mathbf{y})} < \widehat{\gamma} \\ \mathcal{H}_1 \text{ else} \end{cases} \quad (16)$$

where

$$f_{\boldsymbol{\theta}+H(\mathbf{c})}(\mathbf{z}) = \frac{1}{(2\pi)^{\frac{n}{2}}} \exp\left\{-\frac{1}{2}\left\|\mathbf{z} - \boldsymbol{\theta} - H(\mathbf{c})\right\|_2^2\right\} \quad (17)$$

is the probability density function (pdf) of the distribution $\mathcal{N}(\boldsymbol{\theta}+H(\mathbf{c}), I_n)$, the pdf of the distribution $\mathcal{N}(H(\mathbf{c}), I_n)$ is obtained directly from (17) by assuming that $\boldsymbol{\theta} = 0$ and the threshold $\widehat{\gamma}$ is chosen to satisfy the false alarm level α : $\sup_{\mathbf{c}\in K} \Pr_{\boldsymbol{\theta}=0,\mathbf{c}}(\widehat{\Lambda}(\mathbf{y}) \geq \widehat{\gamma}) = \alpha$. But this solution suffers from several disadvantages. First of all, the problem of non-asymptotic optimality of $\widehat{\delta}(\mathbf{y})$ remains unsolved. Under certain regularity assumptions [1], [2], [26], [27], when the number n of observations is arbitrarily large, some optimal properties can be established for the GLR test. But the quality of the GLR test can be questionable for a limited number of observations and even for an arbitrarily large n if the regularity conditions are not satisfied (see a nice discussion in [30]). Indeed, when n is small or moderate, the quality of the GLR test is directly related to the quality of the Maximum Likelihood (ML) estimate $(\widehat{\mathbf{c}}, \widehat{\boldsymbol{\theta}}) = \arg\inf_{\boldsymbol{\theta},\mathbf{c}\in K} \|\mathbf{y} - \boldsymbol{\theta} - H(\mathbf{c})\|_2^2$ (see details in [2]), which is very difficult to evaluate in practice. Second, the numerical realization of the ML procedure meets serious difficulties : a poor and unstable convergence of the minimization process ; a high sensitivity to initial conditions. Our experience with the problem of nuclear fuel rod inspection shows that the numerical application of the GLR test given by (16) leads to poor results.

For this reason, the following approach is developed in the next section : a linearized measurement model and a corresponding optimal test are designed. The proposed test can be interpreted as a linearized GLR test. It does not require to study the nuisance non-linearity and it is also free from any numerical instability, which is very attractive from the practical point of view.

VI. Proposed defect detection algorithm

First, a linearized model of nuisance parameters and corresponding "linearized" GLR test are proposed to overcome the obstacles induced by a non-linear model. Next, a detailed flowchart of defect detection algorithm is presented and discussed.

A. An almost optimal solution

The measurement model given by (12) is non-linear due to the function $r \mapsto F(r)$ which is infinitely differentiable

on the interval $I = [r_0 - \varrho; r_0 + \varrho]$. Therefore, by using the second-order Taylor expansion, the vector function $\mathbf{c} \mapsto H(\mathbf{c})$ can be re-written in the following manner :

$$H(\mathbf{c}) \approx \Sigma^{-\frac{1}{2}} \left[F(r_0) + (r - r_0)\dot{F}(r_0) \right] \mathbf{a} + \Sigma^{-\frac{1}{2}} G\mathbf{b} \quad (18)$$

as $r \to r_0$ where

$$\dot{F}(r) = (F_1'(r) \;\; F_2'(r) \;\; \ldots \;\; F_{n_{\mathbf{a}}}'(r)) \quad (19)$$

is an $n \times n_{\mathbf{a}}$ matrix of first-order derivatives of F and

$$F_s'(r) = \mathrm{vec}\left(\left\{ \frac{dl^s(x_i, y_j; r)}{dr} \right\} \right)$$

for $1 \leq s \leq n_{\mathbf{a}}$. The following linearized model of the non-anomalous background will be used in the rest of the paper :

$$\begin{aligned} H(\mathbf{c}) &\simeq \Sigma^{-\frac{1}{2}} \left[\dot{F}(r_0) \mid F(r_0) \mid G \right] \begin{pmatrix} (r - r_0)\mathbf{a} \\ \mathbf{a} \\ \mathbf{b} \end{pmatrix} \\ &\simeq H_r \mathbf{x}_r. \end{aligned} \quad (20)$$

The peculiarity of this linearized model is the fact that the radius r is artificially replaced by the vector $(r - r_0)\mathbf{a}$ to avoid the simultaneous non-linear estimation of r and $\mathbf{a}$ in the case of GLR (see (16)). Therefore, the components of the vector $\mathbf{x}_r \in \mathbb{R}^{2n_{\mathbf{a}} + n_{\mathbf{b}}}$ are considered as independent variables, ignoring their intrinsic relations in the model of nuisance.

Assuming the linear approximation $H(\mathbf{c}) \simeq H_r \mathbf{x}_r$, the initial problem (14)-(15) becomes tractable. The optimal test, δ_r say, solving this problem is presented in [21]. Let $P_{H_r}^{\perp}$ be the orthogonal projection

$$P_{H_r}^{\perp} = I_n - H_r (H_r^T H_r)^{-1} H_r^T. \quad (21)$$

If the matrix H_r is not full rank then the inverse matrix $(H_r^T H_r)^{-1}$ is replaced by a generalized inverse $(H_r^T H_r)^{-}$ of $(H_r^T H_r)$ [31, Ch. 1.5.3]. The optimal "linearized" test δ_r is simply given by :

$$\delta_r(\mathbf{y}) = \begin{cases} \mathcal{H}_0 \;\text{ if }\; \Lambda_r(\mathbf{y}) = \left\| P_{H_r}^{\perp} \mathbf{y} \right\|_2^2 < \gamma_r \\ \mathcal{H}_1 \;\text{ else} \end{cases}, \quad (22)$$

where the threshold γ_r is chosen to satisfy the probability of false alarm α : $\Pr_{\boldsymbol{\theta}=0}(\Lambda_r(\mathbf{y}) \geq \gamma_r) = \alpha$ (see details in [20]).

To deal with the nuisance parameters there are two different concepts : *i)* the estimation of the nuisance parameters (in order to eliminate their impact) ; *ii)* the direct rejection of the nuisance parameters. There exists a relation between these two concepts. The principal obstacle to implementing the GLR test is a non-linear estimation of the informative $\boldsymbol{\theta}$ and nuisance $\mathbf{c}$ parameters in (16). In contrast to such a non-linear optimization, the rejection of the linearized nuisance is much simpler : the intrinsic dependence between the estimated parameters, which leads to a poor and unstable convergence in the case of the non-linear estimation, is not an obstacle for the nuisance rejection problem which performs even better in the case where the matrix H_r is not full rank. Hence, due to a conveniently chosen linearized nuisance parameter model, the disadvantages of GLR test are transformed in the advantages of the test based on the linear rejection. The price of this transformation is a certain loss of optimality of the "linearized" test δ_r. However, it is shown in [29] that this loss of optimality is negligible.

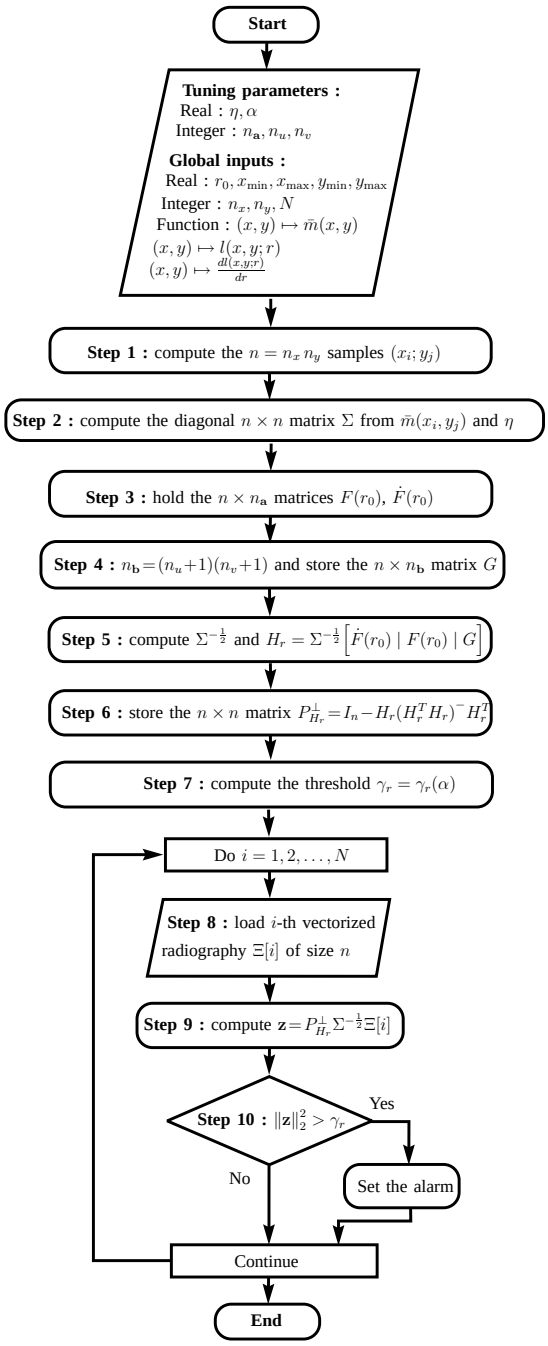

Fig. 3. Flowchart of the detection algorithm.

B. Flowchart of defect detection algorithm

Figure 3 describes the flowchart of the detection algorithm based on the decision rule given by (22). This algorithm can be used to process a certain number (say,

N) of radiographies. The main steps of this flowchart are the following :

Step 1 : definition of vector of the detector sampling coordinates (x_i, y_j) for the region of interest $\mathcal{R}$ taking in the lexicographical order (see (3)).

Step 2 : definition of the diagonal matrix $\Sigma^{-\frac{1}{2}}$ (see (13)). Its diagonal elements are computed by using (8).

Step 3 :calculation of the matrices $F(r_0)$ (see (10)) and $\dot{F}(r_0)$ (see (19)) associated to the mean number of photons passing through the inspected object.

Step 4 : calculation of the matrix G (see (11)) associated to the scattered radiations.

Step 5 : calculation of the matrix H_r (see (20)) associated to the "linearized" measurement model.

Step 6 : calculation of the projection matrix $P^{\perp}_{H_r}$ (see (21)) used to eliminate the unknown background. An alternative and numerically stable solution is to compute an $(n - 2n_{\mathbf{a}} - n_{\mathbf{b}}) \times n$ matrix W such that $W^T W = P^{\perp}_{H}$, $WW^T = I_n$ and $WH_r = 0$ (see details in [20], [21], [28], [29]). It is easy to see that $\left\| P^{\perp}_{H_r} \mathbf{y} \right\|_2^2 = \|W\mathbf{y}\|_2^2$.

Step 7 : calculation of the threshold $\gamma_r = \gamma_r(\alpha)$ as a function of the probability of false alarm α. Under hypothesis $\mathcal{H}_0$, the statistics $\Lambda_r(\mathbf{y})$ is distributed according to the central χ^2 law with $n - 2n_{\mathbf{a}} - n_{\mathbf{b}}$ degrees of freedom. Hence, the threshold can be easily computed by using the χ^2 inverse cumulative distribution function.

Step 8 : starting from this step, a certain number N of radiographies can be processed automatically by using the results of the previous steps. Each radiography viewed as the matrix $\{\zeta_{i,j}\}$ is stored as the vector Ξ taking in the lexicographical order.

Step 9 : first, the i-th vector $\Xi[i]$ is multiplied by a diagonal matrix (see (13)) : $\mathbf{y} = \Sigma^{-\frac{1}{2}} \Xi[i]$. Next, the background is rejected : $\mathbf{z} = P^{\perp}_{H_r} \mathbf{y}$ (or alternatively, $\tilde{\mathbf{z}} = W\mathbf{y}$).

Step 10 : the vector of residuals $\mathbf{z}$ contains only the measurement noise and, eventually, defects. If the squared norm $\|\mathbf{z}\|_2^2$ is greater than the threshold γ_r, then the alarm is set (see (22)).

The orders $n_{\mathbf{a}}$, n_u and n_v of polynomial functions are chosen to optimize the quality of the background rejection. The probability of false alarm α is adjusted to find a trade-off between the sensitivity of the test and the frequency of false alarms. Sometimes, the experimental parameter η can be chosen to artificially increase the variance of the measurement noise and, in such a way, to reduce the impact of the mismatches between the model and the real data on the performances of detection algorithm.

C. Two remarks

First, the function $\mathbf{c} \mapsto H(\mathbf{c})$ which parameterizes the non-anomalous background, is crucially important but there is no general way to design such a parametrization. In practice, a tradeoff between the quality of approximation and its complexity should be established. The main advantage of this approach consists in using a simple "gray-box" model rather than using a complete physical model which takes a long time to be developed and requires serious efforts of experts. Moreover, the detection algorithm is very simple and easily implemented.

Second, another important problem is the anomaly detectability. A detailed discussion on this problem can be found in [20], [21]. The main idea of the parametric approach is that the non-anomalous background (physical/geometrical properties of the nominal fuel rod body) can be approximated by a (non-)linear parametric model : $\mathbf{c} \mapsto H(\mathbf{c})$. Such a parametric model allows us to find a residual subspace where the impact of the non-anomalous background is absent or negligible. Because of the rejection of the unknown non-random background, anomalies can be potentially damaged. For example, the field-flattening operation [5] sometimes leads to the situation where the anomaly becomes undetectable after the application of this operation, which shows the importance of the problem of anomaly detectability for such a non-Bayesian approach. Let the column space of the matrix H_r is denoted by $R(H_r)$ and its orthogonal complement by $R(H_r)^{\perp}$. As it is shown in [21], an anomaly becomes undetectable when the statistical decision rule assimilates the anomaly with the background, which typically occurs when $\boldsymbol{\theta} \in R(H_r)$. Hence, it is assumed that $\boldsymbol{\theta} \in \boldsymbol{\Theta} = R(H_r)^{\perp}$ to warrant the detectability of the anomaly $\boldsymbol{\theta}$. In practice, this assumption is always verified by real anomalies in the case of nuclear fuel rod inspection.

VII. Experiments

The external radius r of a typical fuel rod belongs to the interval $I = [r_0 - \varrho; r_0 + \varrho]$ with $r_0 = 0.47$ cm and $\varrho = 0.005$ cm (relative geometric error of 1%). The region of interest represents a rectangle in the xOy-plane with 0.1653 cm $\leq x \leq 0.3126$ cm and 0.2946 cm $\leq y \leq 0.5922$ cm (see Figure 1). The planar detector, limited to the region of interest, is composed of $n = n_x \times n_y$ sensors, where $n_x = 50$ and $n_y = 100$, i.e. $n = 5\,000$. A typical radiography of the region of interest in the case of non-anomalous background is shown in Figure 4.(a). The coefficient $\eta = 0.1749$ and the mean value of the function $(x, y) \mapsto \bar{m}(x, y)$ in (8) have been established experimentally and by using the a priori information on the geometric properties of a non-anomalous nuclear fuel rod. From the practical considerations, the following degrees of polynomial approximations have been chosen $n_{\mathbf{a}} = 2$ and $n_u = n_v = 3$, i.e. $n_{\mathbf{b}} = 16$. It is assumed that the vector $\mathbf{b}$ is completely unknown and the vector $\mathbf{a} = (a_1 \; a_2)^T$ belongs to the compact set

$$K_{\mathbf{a}} = \big\{(x, y) \in \mathbb{R}^2 \mid \; -2\,000 \leq x \leq 2\,000\,, \\ -20\,000 \leq y \leq 20\,000\big\}\,.$$

As it follows from experiments, a typical value for $\mathbf{a}$ is $(75.23 \;\; -2\,607.7)^T$. The bounds of the compact set $K_{\mathbf{a}}$ are chosen sufficiently large to warrant the stability of the

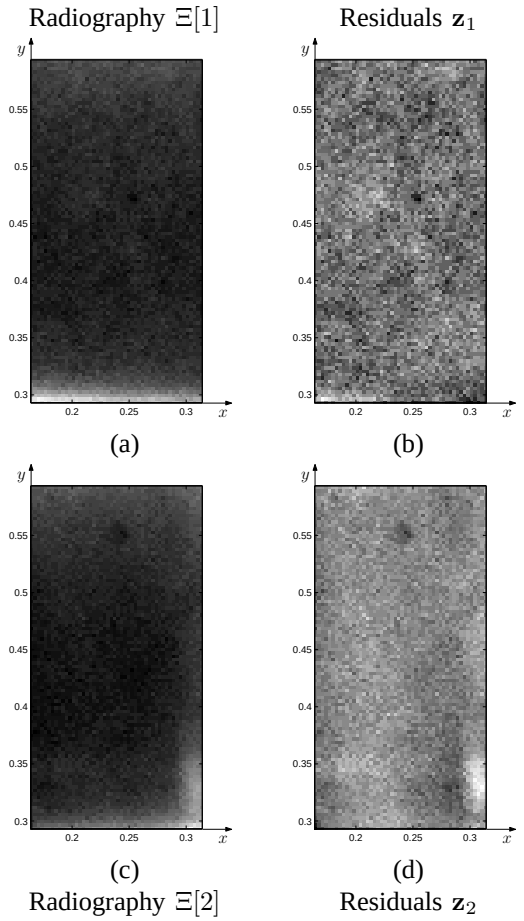

Fig. 4. (a) Radiography $\Xi[1]$ of a non-anomalous fuel rod, (b) residuals $\mathbf{z}_1 = P^{\perp}_{H_r}\Sigma^{-\frac{1}{2}}\Xi[1]$ of the radiography (a), (c) radiography $\Xi[2]$ of a fuel rod with an anomaly, (d) residuals $\mathbf{z}_2 = P^{\perp}_{H_r}\Sigma^{-\frac{1}{2}}\Xi[2]$ of the radiography (c).

decision algorithm against this parameter. The matrix H_r is full column rank.

The radiography $\Xi[1]$ on Figure 4(a) corresponds to an anomaly-free inspected nuclear fuel rod. The proposed method efficiently rejects the unknown background and produces the residuals that are close to a "white noise" (see Figure 4(b)). The probability of false alarm is fixed at 10^{-2} and, consequently, the threshold has been chosen as $\gamma_r = 5\,222.27$. The decision function is $\Lambda_r(\mathbf{y}_1) = 4\,986.02 < \gamma_r$. The hypothesis $\mathcal{H}_0$ is accepted. Figure 4(c) presents a radiography $\Xi[2]$ with an anomaly. This leads to the residuals with an "anomaly signature" (white and black spots) shown in Figure 4(d). The decision function is $\Lambda_r(\mathbf{y}_2) = 7\,152.40 > \gamma_r$ and the hypothesis $\mathcal{H}_1$ is accepted.

VIII. Conclusion

The non-Bayesian detection of an anomaly from a single or a few noisy tomographic projections is considered as a statistical hypotheses testing problem. Some insight in the problem of nuclear fuel rod inspection is given in section II. The state of the art, the motivation of this study and the main contribution of the paper are given in section III. In section IV, a parametric parsimonious model is proposed to describe the non-anomalous manufactured object with two types of uncertainty : the geometrical imprecisions and the parametric uncertainty in beam hardening and X-ray scattering models. The limits of the well-known non-linear GLR test are discussed in section V. A new detection scheme based on the "linearized" optimal test is proposed in section VI as an alternative to the non-linear GLR test, which is untractable in the above-mentioned context. The experimental results on real radiographic data confirm the relevance and efficiency of the proposed solution in section VII.

References

[1] A. Wald, "Tests of statistical hypotheses concerning several parameters when the number of observations is large," *Trans. Amer. Math. Soc.*, vol. 54, pp. 426–482, 1943.

[2] G. A. F. Seber and C. J. Wild, *Nonlinear regression*. Wiley, 1989.

[3] F. Retraint, "Contrôle non destructif de pièces industrielles par radiographie : caractérisation quantitative et reconstruction 3D à partir d'un nombre limité de vues," PhD dissertation, INSA-Lyon, 1998.

[4] D. Mery, T. Jaeger, and D. Filbert, "A review of methods for automated recognition of casting defects," *Journal of The British Institute of Non-Destructive Testing*, vol. 44, no. 7, pp. 428–436, 2002.

[5] L. E. Bryant, *Nondestructive tesing handbook (second edition)*. American Society for Nondestructive Testing, 1985, vol. 3 : radiography & testing.

[6] H. Boerner and H. Strecker, "Automated x-ray inspection of aluminium casting," *IEEE Trans. Pattern Anal. Machine Intell.*, vol. 10, no. 1, pp. 79–91, 1988.

[7] A. Kehoe and G. Parker, "An intelligent knowledge based approach for the automated radiographic inspection of castings," *NDT&E International*, vol. 25, no. 1, pp. 23–36, 1992.

[8] S. Lawson and G. Parker, "Intelligent segmentation of industrial radiographic images using neural networks," in *Machine Vision Applications ans Systems Integration III, Proc. of SPIE*, vol. 2347, 1994, pp. 245–255.

[9] G. Wang and T. W. Liao, "Automatic identification of different types of welding defects in radiographic images," *NDT&E International*, vol. 35, no. 8, pp. 519–528, 2002.

[10] A. Gayer, A. Saya, and A. Shiloh, "Automatic recognition of welding defects in real-time radiography," *NDT International*, vol. 23, no. 4, pp. 131–136, 1990.

[11] D. Mery and D. Filbert, "Automated flaw detection in aluminum castings based on the tracking of potential defects in a radioscopic image sequence," *IEEE Trans. Robot. Automat.*, vol. 18, no. 6, pp. 890–901, 2002.

[12] K. Castleman, *Digital Image Processing*, 2nd ed. Prentice-Hall, 1996.

[13] F. Natterer, *The Mathematics Of Computerized Tomography*. John Wiley & Sons, 1986.

[14] G. Demoment, "Image reconstruction and restoration : overview of common estimation structures and problems," *IEEE Trans. Acoust., Speech, Signal Processing*, vol. 37, no. 12, pp. 2024–2036, 1989.

[15] M. Davidson, "The ill-conditionned nature of the limited angle tomography problem," *SIAM Journal of applied mathematics*, vol. 42, no. 3, pp. 428–448, 1983.

[16] E. Miller and A. Willsky, "Multiscale, statistical anomaly detection analysis and algorithms for linearized inverse scattering problems," *Multidimensional Systems and Signal Processing*, vol. 8, pp. 151–184, 1997.

[17] J. Idier (Ed.), *Approche bayésienne pour les problèmes inverses*, ser. Traitement du signal et de l'image. Hermès, Lavoisier (Traité IC2), 2001.

[18] H. H. Barrett and K. J. Myers, *Foundations of Image Science*. John Wiley & Sons, 2004.

[19] A. Frakt, W. Karl, and A. Willsky, "A multiscale hypothesis testing approach to anomaly detection and localization from noisy tomographic data," *IEEE Trans. Image Processing*, vol. 7, no. 6, pp. 825–837, june 1998.

[20] L. Fillatre and I. Nikiforov, "A statistical detection of an anomaly from a few noisy tomographic projections," *Journal of Applied Signal Processing, Special issue on advances in intelligent vision systems : methods and applications-Part II*, no. 14, pp. 2215–2228, 2005.

[21] ——, "Non-bayesian detection and detectability of anomalies from a few noisy tomographic projections," *IEEE Trans. Signal Processing*, vol. 55, no. 2, pp. 401–413, 2007.

[22] I. Kazantsev, I. Lemahieu, G. Salov, and R. Denys, "Statistical detection of defects in radiographic images in nondestructive testing," *Signal Processing*, vol. 82, no. 5, pp. 791–801, 2002.

[23] I. Elbakri and J. Fessler, "Statistical image for reconstruction for polyenergetic x-ray computed tomography," *IEEE Trans. Med. Imag.*, vol. 21, no. 2, pp. 89–99, 2002.

[24] G. T. Herman, "Correction for beam hardening in computed tomography," *Phys. med. biol.*, vol. 24, no. 1, pp. 81–106, 1979.

[25] H. Barret and W. Swindell, *Radiological Imaging*. New York Academic, 1981.

[26] A. A. Borovkov, *Mathematical Statistics*. Gordon and Breach Sciences Publishers, Amsterdam, 1998.

[27] E. Lehman, *Testing Statistical Hypotheses, Second Edition*. Chapman & Hall, 1986.

[28] M. Fouladirad and I. Nikiforov, "Optimal statistical fault detection with nuisance parameters," *Automatica*, vol. 41, no. 7, pp. 1157 – 1171, jul 2005.

[29] L. Fillatre, I. Nikiforov, and F. Retraint, "ε-optimal non-bayesian anomaly detection for parametric tomography," in *IEEE Trans. Image Processing*, 2007, submitted.

[30] B. Porat and B. Friedlander, "On the generalized likelihood ratio test for a class of nonlinear detection problems," *IEEE Trans. Signal Processing*, vol. 41, no. 11, pp. 3186–3190, 1993.

[31] K.-R. Koch, *Parameter estimation and hypothesis testing in linear models*. Springer-Verlag, Berlin, Heidelberg, New York, 1999.

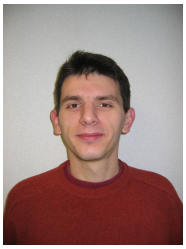

Lionel Fillatre received the M.Sc. degree in decision and information engineering and the Ph.D. degree in systems optimization from the University of Technology of Troyes (UTT), France, in 2001 and 2004, respectively. He is currently an associate professor at the UTT. His current research interests include statistical decision theory, signal and image processing, non-destructive testing and statistical characterization of traffic flows in telecommunications networks.

Igor Nikiforov received his M.S. degree in automatic control from the Moscow Physical - Technical Institute in 1974, and the Ph.D. in automatic control from the Institute of Control Sciences (USSR Academy of Science), Moscow, in 1981. He joined the University of Technology of Troyes (UTT) in 1995, where he is Professor and Head of the system modeling and dependability laboratory (LM2S) which is a part of the Institute of Charles Delaunay, FRE CNRS 2848. His scientific interests include statistical decision theory, detection/isolation of abrupt changes, fault detection/isolation/reconfiguration, signal processing and navigation.

Florent Retraint received the M.Sc. degree in applied mathematics and the Ph.D. degree in image processing from the National Institute of Applied Sciences of Lyon, France, in 1994 and 1997, respectively. He is currently an associate professor at the University of Technology of Troyes. His current research interests include statistical decision theory, image processing, non-destructive testing.